Eigenvalue Tracking of Large-Scale Systems Impacted by Time Delays

Andreas Bouterakos, Georgios Tzounas, *Member, IEEE*

Abstract—The paper focuses on tracking eigenvalue trajectories in power system models with time delays. We formulate a continuation-based approach that employs numerical integration to follow eigenvalues as system parameters vary, in the presence of one or multiple delayed variables. The formulation is compatible with sparse delay differential-algebraic equation (DDAE) formulations of the system model and allows treating the delay magnitude itself as a varying parameter with implementation aspects discussed in detail. The proposed approach is illustrated on a modified IEEE 39-bus system, as well as on a real-world-scale dynamic model of the Irish transmission network.

Index Terms—Continuation methods, eigenvalue tracking, small-signal stability analysis (SSSA), time delays.

I. INTRODUCTION

A. Motivation

TIME delays, arising from the growing volume of data processing and communication in inverter-dominated grids, are an increasingly important factor influencing power system dynamics. In particular, when present in closed-loop control settings, time delays can weaken damping and reduce the system's stability margin [1]–[5]. These effects can be readily assessed using small-signal stability analysis (SSSA), where eigenvalue analysis plays a central role [6]. However, when delays are present, eigenvalue computations and tracking become more involved, particularly in large-scale systems. This paper focuses on continuation-based methods for tracking eigenvalues in power system models with time delays.

B. Literature Review

Power system dynamics are commonly modeled through a set of differential-algebraic equations (DAEs) [7]. Introducing time delays transforms the model into delay differential-algebraic equations (DDAEs). In the context of SSSA, the stability of linearized DAEs and DDAEs is determined by their eigenvalues, defined as the roots of the system's characteristic equation. For DDAEs, this equation is transcendental and gives rise to infinitely many eigenvalues [6]. Approximation techniques such as Padé polynomials or spectral discretization yield a finite-dimensional linear eigenvalue problem, which can then be solved using standard numerical algorithms [8].

These include dense-matrix methods (e.g., QR or QZ) for small to medium-sized systems, and sparse techniques (e.g., Krylov) for large-scale cases. However, when tracking eigenvalue trajectories as system parameters vary, repeated use of these solvers can be either computationally expensive or challenging to apply in a fully automated setting.

Continuation-based methods have been proposed as an alternative framework for tracking eigenvalue trajectories more efficiently. The core idea of continuation methods is to incrementally update the solution of a parameter-dependent problem using previously computed values. In the context of eigenvalue tracking, this solution consists of a subset of the system's eigenpairs, i.e., eigenvalues with their associated eigenvectors. For dynamical systems without time delays, [9] proposes a continuation-based algorithm that employs Newton's method to follow eigenvalue trajectories, highlighting the benefits of including a predictor step before each iteration. The authors in [10] combine this approach with a Cayley transform that updates the dimension of the considered subspace at every iteration, focusing the computation on the modes most critical for stability. To evaluate stability margins of power systems, [11] derives eigenvalue and eigenvector sensitivities with respect to varying parameters and traces their trajectories through numerical integration. This approach makes it possible to identify poorly damped modes, in particular those that are critical for system stability.

Despite the aforementioned advances in continuation-based tracking, only a very limited number of works have taken into account time delays. Among them, [12] uses the derivatives of the characteristic equation with respect to system parameters to formulate a Sylvester-type matrix equation. The resulting tangent approximation enables eigenpair tracking but requires elimination of algebraic variables, restricting applicability to small and medium-sized power systems. In contrast, [13] formulates eigen-sensitivities and tracking directly on the DDAE model, thereby retaining the sparsity structure. In that work, the incremental updates of the eigenpairs are obtained through Newton iterations, which may be sensitive to discontinuities and poor initialization (e.g., see [14]). Finally, existing works exclusively consider constant delays, effectively neglecting real-world communication network effects such as noise and data packet dropouts.

C. Contribution

This paper develops a continuation-based tracking formulation for power system models described by DDAEs. The formulation permits multiple parameters to vary simultaneously

and allows the delay magnitude to be treated as a continuation parameter, enabling an accurate estimation of stability margins. Extension to account for real-world communication network effects, such as noise and data packet dropouts, is also discussed. These contributions are demonstrated through a comprehensive case study. First, the method is applied to systems with a single and multiple delays, tracking eigenvalues with respect to parameter variations. Second, the formulation considers the magnitude of the time delay as the varying parameter and its accuracy in capturing the stability margin is demonstrated. Finally, computational aspects are assessed on a large-scale dynamic model of the all-island Irish transmission network.

D. Paper Organization

The remainder of the paper is organized as follows. Section II introduces preliminaries on SSSA. Section III discusses the formulation and implementation aspects of the proposed eigenvalue tracking approach. Section IV presents simulation results, based on the modified 39-bus system and a real-world scale model of the Irish transmission system, highlighting the validity of the method. Finally, Section V draws conclusions and outlines directions for future work.

II. SMALL-SIGNAL STABILITY ANALYSIS

A. DDAE Power System Model

Short-term power system stability in the presence of delays can be studied through a set of nonlinear DDAEs in semi-implicit[1] form [6]:

$$\begin{bmatrix} \boldsymbol{T} & \boldsymbol{0}_{n,m} \\ \boldsymbol{R} & \boldsymbol{0}_{m,m} \end{bmatrix} \begin{bmatrix} \boldsymbol{x}' \\ \boldsymbol{y}' \end{bmatrix} = \begin{bmatrix} \boldsymbol{f}(\boldsymbol{x}, \boldsymbol{y}, \boldsymbol{x}_d, \boldsymbol{y}_d) \\ \boldsymbol{g}(\boldsymbol{x}, \boldsymbol{y}, \boldsymbol{x}_d, \boldsymbol{y}_d) \end{bmatrix} \quad (1)$$

where $\boldsymbol{x} = \boldsymbol{x}(t) : [0, \infty) \to \mathbb{R}^n$ are the states of dynamic devices such as generators, dynamic loads, and controllers; $\boldsymbol{y} = \boldsymbol{y}(t) : [0, \infty) \to \mathbb{R}^m$ are algebraic variables associated with network equations and auxiliary control setpoints; $\boldsymbol{f}$ and $\boldsymbol{g}$ are nonlinear functions; $\boldsymbol{T} \in \mathbb{R}^{n \times n}$, $\boldsymbol{R} \in \mathbb{R}^{m \times n}$; and $\boldsymbol{0}_{n,m}$ denotes the $n \times m$ zero matrix. The delayed state and algebraic variables are denoted as $\boldsymbol{x}_d$ and $\boldsymbol{y}_d$, with:

$$\begin{aligned} \boldsymbol{x}_d(t) &= \{\boldsymbol{x}(t - \tau_1), \boldsymbol{x}(t - \tau_2), \dots, \boldsymbol{x}(t - \tau_\mu)\} \\ \boldsymbol{y}_d(t) &= \{\boldsymbol{y}(t - \tau_1), \boldsymbol{y}(t - \tau_2), \dots, \boldsymbol{y}(t - \tau_\mu)\} \end{aligned} \quad (2)$$

where $\tau_j > 0$, $j = 1, 2, \dots, \mu$, denotes the j-th delay and μ is the total number of delays. For brevity, we denote the j-th delayed variable as:

$$\begin{aligned} \boldsymbol{x}_d^j &= \boldsymbol{x}(t - \tau_j) \;, \\ \boldsymbol{y}_d^j &= \boldsymbol{y}(t - \tau_j) \;, \end{aligned} \quad (3)$$

where $j = 1, 2, \dots, \mu$.

[1]The semi-implicit form is often adopted because it can offer certain practical advantages, such as increased sparsity as well as flexibility in handling state and algebraic variables, see [6].

B. Eigenvalue Analysis

To study how the system responds to parameter variations, we introduce a scalar continuation parameter $p \in \mathbb{R}$, used to parametrize selected system quantities of interest. Then, (1) is rewritten as follows:

$$\begin{bmatrix} \boldsymbol{T}(p) & \boldsymbol{0}_{n,m} \\ \boldsymbol{R}(p) & \boldsymbol{0}_{m,m} \end{bmatrix} \begin{bmatrix} \boldsymbol{x}' \\ \boldsymbol{y}' \end{bmatrix} = \begin{bmatrix} \boldsymbol{f}(\boldsymbol{x}, \boldsymbol{y}, \boldsymbol{x}_d, \boldsymbol{y}_d, p) \\ \boldsymbol{g}(\boldsymbol{x}, \boldsymbol{y}, \boldsymbol{x}_d, \boldsymbol{y}_d, p) \end{bmatrix} \quad (4)$$

An equilibrium $(\boldsymbol{x}_o, \boldsymbol{y}_o) := [\boldsymbol{x}_o^\mathsf{T}, \boldsymbol{y}_o^\mathsf{T}]$ (T indicating the transpose) of (4) is defined assuming the system has been at rest for time equal or larger than the maximum delay. Considering small disturbances, (4) can be linearized around the equilibrium, as follows:

$$\begin{aligned} \begin{bmatrix} \boldsymbol{T}(p) & \boldsymbol{0}_{n,m} \\ \boldsymbol{R}(p) & \boldsymbol{0}_{m,m} \end{bmatrix} \begin{bmatrix} \Delta\boldsymbol{x}' \\ \Delta\boldsymbol{y}' \end{bmatrix} &= \begin{bmatrix} \boldsymbol{f}_x(p) & \boldsymbol{f}_y(p) \\ \boldsymbol{g}_x(p) & \boldsymbol{g}_y(p) \end{bmatrix} \begin{bmatrix} \Delta\boldsymbol{x} \\ \Delta\boldsymbol{y} \end{bmatrix} \\ &+ \sum_{j=1}^{\mu} \left(\begin{bmatrix} \boldsymbol{f}_{x,j}(p) & \boldsymbol{f}_{y,j}(p) \\ \boldsymbol{g}_{x,j}(p) & \boldsymbol{g}_{y,j}(p) \end{bmatrix} \begin{bmatrix} \Delta\boldsymbol{x}_d^j \\ \Delta\boldsymbol{y}_d^j \end{bmatrix} \right) \end{aligned} \quad (5)$$

where $\Delta\boldsymbol{x} = \boldsymbol{x} - \boldsymbol{x}_o$, $\Delta\boldsymbol{y} = \boldsymbol{y} - \boldsymbol{y}_o$; $\boldsymbol{f}_x$, $\boldsymbol{f}_y$, $\boldsymbol{g}_x$, $\boldsymbol{g}_y$ and $\boldsymbol{f}_{x,j}$, $\boldsymbol{f}_{y,j}$, $\boldsymbol{g}_{x,j}$, $\boldsymbol{g}_{y,j}$ are the delay-free and delayed Jacobians, respectively, evaluated at $(\boldsymbol{x}_o, \boldsymbol{y}_o)$. Equation (5) is of the form:

$$\mathbf{E}(p)\,\mathbf{x}' = \mathbf{A}_0(p)\,\mathbf{x} + \sum_{j=1}^{\mu} \mathbf{A}_j(p)\,\mathbf{x}_d^j \quad (6)$$

where

$$\mathbf{x} = (\Delta\boldsymbol{x}, \Delta\boldsymbol{y})\;,$$
$$\mathbf{x}_d^j = (\Delta\boldsymbol{x}_d^j, \Delta\boldsymbol{y}_d^j)\;,$$

and

$$\begin{aligned} \mathbf{E}(p) &\equiv \begin{bmatrix} \boldsymbol{T}(p) & \boldsymbol{0}_{n,m} \\ \boldsymbol{R}(p) & \boldsymbol{0}_{m,m} \end{bmatrix}, \quad \mathbf{A}_0(p) \equiv \begin{bmatrix} \boldsymbol{f}_x(p) & \boldsymbol{f}_y(p) \\ \boldsymbol{g}_x(p) & \boldsymbol{g}_y(p) \end{bmatrix} \\ \mathbf{A}_j(p) &\equiv \begin{bmatrix} \boldsymbol{f}_{x,j}(p) & \boldsymbol{f}_{y,j}(p) \\ \boldsymbol{g}_{x,j}(p) & \boldsymbol{g}_{y,j}(p) \end{bmatrix} \end{aligned} \quad (7)$$

Applying the Laplace transform to (6):

$$\left(s\mathbf{E}(p) - \mathbf{A}_0(p) - \sum_{j=1}^{\mu} \mathbf{A}_j(p)e^{-s\tau_j}\right) \mathcal{L}\{\mathbf{x}\} = \mathbf{E}(p)\mathbf{x}(0) \quad (8)$$

where s is a complex variable in the S-plane. The associated eigenvalue problem is:

$$\mathbf{P}(s, p)\,\boldsymbol{\phi} = \mathbf{0}_{r,1}\;, \quad r = n + m \quad (9)$$

where any value of s that satisfies (9) is an eigenvalue of the matrix function:

$$\mathbf{P}(s, p) = s\mathbf{E}(p) - \mathbf{A}_0(p) - \sum_{j=1}^{\mu} \mathbf{A}_j(p)e^{-s\tau_j} \quad (10)$$

with $\boldsymbol{\phi}$ being the associated right eigenvector. The matrix function $\mathbf{P}(s, p)$ plays an important role in the stability and dynamic behavior of (6).

III. Eigenvalue Tracking

This section presents a continuation-based approach for tracking the eigenvalues of power systems with time delays. The method is first introduced for the case of a single delayed variable, then generalized to systems with multiple delays, and extended to allow the delay magnitude itself to vary as the continuation parameter. Handling stochastic, time-varying communication delays is also duly discussed.

A. Tracking in the Presence of a Single Delay

We begin with the case of a single delay $\tau = \tau_1$ ($\mu = 1$). In this case, (10) takes the form:

$$\mathbf{P} = s\mathbf{E} - \mathbf{A}_0 - \mathbf{A}_1 e^{-s\tau} \tag{11}$$

where the dependence on p is omitted for brevity. Differentiation of (9) with respect to p gives:

$$\dot{\mathbf{P}}\,\phi + \mathbf{P}\,\dot{\phi} = \mathbf{0}_{r,1} \tag{12}$$

where

$$\dot{\mathbf{P}} = \dot{s}\mathbf{E} + s\dot{\mathbf{E}} - \dot{\mathbf{A}}_0 - \dot{\mathbf{A}}_1 e^{-s\tau} + \tau\dot{s}\mathbf{A}_1 e^{-s\tau} \tag{13}$$

with:

$$\dot{s} = \partial s/\partial p \,, \quad \dot{\mathbf{E}} = \partial\mathbf{E}/\partial p \,, \quad \dot{\mathbf{A}}_0 = \partial\mathbf{A}_0/\partial p \,,$$
$$\dot{\mathbf{A}}_1 = \partial\mathbf{A}_1/\partial p \,, \quad \dot{\phi} = \partial\phi/\partial p.$$

Equivalently, equation (12) is:

$$(s\mathbf{E} - \mathbf{A}_0 - \mathbf{A}_1 e^{-s\tau})\dot{\phi} + (\mathbf{E} + \tau\mathbf{A}_1 e^{-s\tau})\phi\dot{s} = \\ -(s\dot{\mathbf{E}} - \dot{\mathbf{A}}_0 - \dot{\mathbf{A}}_1 e^{-s\tau})\phi \tag{14}$$

System (14), which describes the evolution of a single eigenpair with respect to p, consists of r equations and $r+1$ unknowns, s and ϕ. To make this system well-posed, it is closed by imposing the following eigenvector normalization:

$$\phi^\mathsf{T}\phi = c \tag{15}$$

where c is an imposed constant, e.g., $c = 1$. Differentiation of (15) gives:

$$\phi^\mathsf{T}\dot{\phi} = 0 \tag{16}$$

Combining (14) and (16):

$$\begin{bmatrix} s\mathbf{E} - \mathbf{A}_0 - \mathbf{A}_1 e^{-s\tau} & (\mathbf{E} + \tau\mathbf{A}_1 e^{-s\tau})\phi \\ \phi^\mathsf{T} & 0 \end{bmatrix}\begin{bmatrix} \dot{\phi} \\ \dot{s} \end{bmatrix} = \\ \begin{bmatrix} -(s\dot{\mathbf{E}} - \dot{\mathbf{A}}_0 - \dot{\mathbf{A}}_1 e^{-s\tau})\phi \\ 0 \end{bmatrix} \tag{17}$$

Splitting real and imaginary parts, i.e.

$$\phi = \phi_\mathrm{r} + \jmath\phi_\mathrm{i} \,,$$
$$s = s_\mathrm{r} + \jmath s_\mathrm{i} \,,$$

and by setting $\mathbf{A}_1 e^{-s_\mathrm{r}\tau}\cos(s_\mathrm{i}\tau) = \mathbf{C}$, $\mathbf{A}_1 e^{-s_\mathrm{r}\tau}\sin(s_\mathrm{i}\tau) = \mathbf{S}$, $\dot{\mathbf{A}}_1 e^{-s_\mathrm{r}\tau}\cos(s_\mathrm{i}\tau) = \mathbf{C}_D$ and $\dot{\mathbf{A}}_1 e^{-s_\mathrm{r}\tau}\sin(s_\mathrm{i}\tau) = \mathbf{S}_D$ we arrive at the following system:

$$\mathbf{M}(\mathbf{y})\,\dot{\mathbf{y}} = \mathbf{h}(\mathbf{y}) \tag{18}$$

where $\mathbf{y} = \mathbf{y}(p) = (\phi_\mathrm{r}, \phi_\mathrm{i}, s_\mathrm{r}, s_\mathrm{i})$, with $\mathbf{y} \in \mathbb{R}^{2r+2}$; and:

$$\mathbf{M}(\mathbf{y}) = \begin{bmatrix} \mathbf{M}_1 & \mathbf{M}_2 \\ \mathbf{M}_3 & \mathbf{0}_{2,2} \end{bmatrix}$$

The quantities $\mathbf{h}$, $\mathbf{M}_1$, $\mathbf{M}_2$, $\mathbf{M}_3$ are in this case defined as:

$$\mathbf{h} = \begin{bmatrix} (-s_\mathrm{r}\dot{\mathbf{E}} + \dot{\mathbf{A}}_0 + \mathbf{C}_D)\phi_\mathrm{r} + (s_\mathrm{i}\dot{\mathbf{E}} + \mathbf{S}_D)\phi_\mathrm{i} \\ -(s_\mathrm{i}\dot{\mathbf{E}} + \mathbf{S}_D)\phi_\mathrm{r} + (-s_\mathrm{r}\dot{\mathbf{E}} + \dot{\mathbf{A}}_0 + \mathbf{C}_D)\phi_\mathrm{i} \\ 0 \\ 0 \end{bmatrix}$$

$$\mathbf{M}_1 = \begin{bmatrix} s_\mathrm{r}\mathbf{E} - \mathbf{A}_0 - \mathbf{C} & -s_\mathrm{i}\mathbf{E} - \mathbf{S} \\ s_\mathrm{i}\mathbf{E} + \mathbf{S} & s_\mathrm{r}\mathbf{E} - \mathbf{A}_0 - \mathbf{C} \end{bmatrix}$$

$$\mathbf{M}_2 = \begin{bmatrix} \mathbf{E}\phi_\mathrm{r} + \tau(\mathbf{C}\phi_\mathrm{r} + \mathbf{S}\phi_\mathrm{i}) & -\mathbf{E}\phi_\mathrm{i} - \tau(\mathbf{C}\phi_\mathrm{r} - \mathbf{S}\phi_\mathrm{i}) \\ \mathbf{E}\phi_\mathrm{i} + \tau(\mathbf{C}\phi_\mathrm{r} - \mathbf{S}\phi_\mathrm{i}) & \mathbf{E}\phi_\mathrm{r} + \tau(\mathbf{C}\phi_\mathrm{r} + \mathbf{S}\phi_\mathrm{i}) \end{bmatrix}$$

$$\mathbf{M}_3 = \begin{bmatrix} \phi_\mathrm{r}^\mathsf{T} & -\phi_\mathrm{i}^\mathsf{T} \\ \phi_\mathrm{i}^\mathsf{T} & \phi_\mathrm{r}^\mathsf{T} \end{bmatrix}$$

B. Generalization to Multiple Delays

When multiple delays are present in the system, the expression (12) holds, where in this case the matrix function $\mathbf{P}$ is given by (10). Differentiating (10) with respect to the continuation parameter p gives:

$$\dot{\mathbf{P}} = \dot{s}\mathbf{E} + s\dot{\mathbf{E}} - \dot{\mathbf{A}}_0 - \sum_{j=1}^{\mu}(\dot{\mathbf{A}}_j - \tau_j\dot{s}\mathbf{A}_j)e^{-s\tau_j} \tag{19}$$

Substituting into (12) yields:

$$(\mathbf{E} + \sum_{j=1}^{\mu}\tau_j\mathbf{A}_j e^{-s\tau_j})\phi\dot{s} + (s\mathbf{E} - \mathbf{A}_0 - \sum_{j=1}^{\mu}\mathbf{A}_j e^{-s\tau_j})\dot{\phi} \\ = -(s\dot{\mathbf{E}} - \dot{\mathbf{A}}_0 - \sum_{j=1}^{\mu}\dot{\mathbf{A}}_j e^{-s\tau_j})\phi \tag{20}$$

Combining with (16) and splitting eigenvalue and eigenvector into real and imaginary parts leads to a system in the form of (18), where $\mathbf{M}$ and $\mathbf{h}$ are defined to account for all μ delays. Their detailed definitions are provided in the Appendix.

C. Delay Magnitude as Varying Parameter

In this subsection, we track the evolution of eigenvalues as the delay magnitude is varied. We first consider the case where the system contains a single delayed variable, whose time delay has a varying magnitude and is denoted by τ_ℓ. The corresponding delayed state matrix is denoted by $\mathbf{A}_\ell$. Given $p = \tau_\ell$, the matrix function $\mathbf{P}$ is:

$$\mathbf{P} = s\mathbf{E} - \mathbf{A}_0 - \mathbf{A}_\ell e^{-sp} \tag{21}$$

Matrices $\mathbf{E}$, $\mathbf{A}_0$ and $\mathbf{A}_\ell$ do not explicitly depend on τ, hence differentiation of (21) with respect to p yields:

$$\dot{\mathbf{P}} = \dot{s}\mathbf{E} + \mathbf{A}_\ell(\dot{s}p + s)e^{-sp}$$

Substituting into (12) yields:

$$(s\mathbf{E} - \mathbf{A}_0 - \mathbf{A}_\ell e^{-sp})\dot{\phi} + (\mathbf{E} + \mathbf{A}_\ell p e^{-sp})\phi\dot{s} = -\mathbf{A}_\ell e^{-sp}s\phi \tag{22}$$

By splitting real and imaginary parts of (22), we arrive at a system in the form of (18), where $\mathbf{M}$ and $\mathbf{h}$ are in this

case functions of the varying delay magnitude $p = \tau_\ell$. Their definitions are detailed in the Appendix.

We extend the above formulation to systems with multiple delays, treating one of them as the continuation parameter, i.e., $\tau_\ell = p$. The definition of $\mathbf{P}$ in this case is as follows:

$$\mathbf{P} = s\mathbf{E} - \mathbf{A}_0 - \sum_{j=1}^{\mu} \mathbf{A}_j e^{-s\tau_j} - \mathbf{A}_\ell e^{-sp} \tag{23}$$

We note that the term corresponding to τ_ℓ is kept separate, even if τ_ℓ equals some τ_j, $j = 1, 2, \ldots, \mu$. Given that the matrices $\mathbf{E}$, $\mathbf{A}_0$, $\mathbf{A}_\ell$ and $\mathbf{A}_j$ do not explicitly depend on τ_ℓ, the derivative of (23) with respect to p is:

$$\dot{\mathbf{P}} = \dot{s}\mathbf{E} + \sum_{j=1}^{\mu} \tau_j \dot{s} \mathbf{A}_j e^{-s\tau_j} + \mathbf{A}_\ell (\dot{s}p + s) e^{-sp} \tag{24}$$

and (12) is equivalently written as:

$$(s\mathbf{E} - \mathbf{A}_0 - \mathbf{A}_\ell e^{-sp} - \sum_{j=1}^{\mu} \mathbf{A}_j e^{-s\tau_j})\dot{\phi} +$$

$$(\mathbf{E} + \mathbf{A}_\ell\, p\, e^{-sp} + \sum_{j=1}^{\mu} \tau_j \mathbf{A}_j e^{-s\tau_j})\phi\dot{s} = -\mathbf{A}_\ell e^{-sp} s\phi \tag{25}$$

By splitting the eigenvalue and eigenvector into real and imaginary parts we arrive at a system in the form of (18). The derivation of $\mathbf{M}$ and $\mathbf{h}$ is provided in the Appendix.

D. Communication Delays with Noise and Data Dropouts

The derivations above consider constant delays. In this section, we show how they can be generalized to capture the effects of realistic wide area measurement system (WAMS) latencies with noise and data packet dropouts. To this end, we consider the composite time-varying delay model proposed in [1], in which, for the purpose of SSSA, packet dropouts and noise are captured through the functions $h_p(s)$ and $h_s(s)$, respectively:

$$h_p(s) = \frac{1 - p_{dr}}{s}\left[1 + (p_{dr} - 1)\frac{e^{-sT}}{1 - p_{dr}e^{-sT}}\right] \tag{26}$$

$$h_s(s) = (1 + \frac{\alpha}{1 - p_{dr}}s)^{-b} \tag{27}$$

where α and b are the scale and shape factors of the *Gamma distribution*; p_{dr} is the packet dropout rate; and T is the normal delivery period for each data packet.

Equation (10) takes the adjusted form:

$$\mathbf{P} = s\mathbf{E} - \mathbf{A}_0 - h_p(s)h_s(s)\mathbf{A}_1 e^{-s\tau_0} \tag{28}$$

where τ_0 is the constant component of the WAMS delay. By setting $\mathrm{S}_T = h_p(s)h_s(s)e^{-s\tau_0}$, the derivative of (28) with respect to p is:

$$\dot{\mathbf{P}} = \dot{s}\mathbf{E} + s\dot{\mathbf{E}} - \dot{\mathbf{A}}_0 - \dot{\mathrm{S}}_T\mathbf{A}_1 - \mathrm{S}_T\dot{\mathbf{A}}_1 \tag{29}$$

where

$$\dot{\mathrm{S}}_T = (\frac{\partial h_p}{\partial s}h_s + h_p\frac{\partial h_s}{\partial s} - \tau_0 h_p h_s)e^{-s\tau_0}\dot{s} \\ = \mathrm{S}_{TD}\dot{s} \tag{30}$$

We note that in the case of a constant delay, i.e., $\tau(t) = \tau_0$, it is trivial to deduce from [1] that $h_p(s) = h_s(s) = 1$ and $\partial h_p/\partial s = \partial h_s/\partial s = 0$; therefore, equations (28) and (29) are simplified to (11) and (13) respectively.

Substituting (28) and (29) into (12) yields:

$$(s\mathbf{E} - \mathbf{A}_0 - \mathrm{S}_T\mathbf{A}_1)\dot{\phi} + (\mathbf{E} - \mathrm{S}_{TD}\mathbf{A}_1)\phi\dot{s} = \\ -(s\dot{\mathbf{E}} - \dot{\mathbf{A}}_0 - \mathrm{S}_T\dot{\mathbf{A}}_1)\phi \tag{31}$$

By splitting real and imaginary parts of (31), we arrive at a system in the form of (18), where the definitions of $\mathbf{M}$ and $\mathbf{h}$ are detailed in the Appendix.

E. Numerical Integration

Given a parameter range $[p_{init}, p_{fin}]$, tracking is performed by numerically integrating (18). For the initial value p_{init}, the state vector $\mathbf{y}(p_{init})$ is obtained by solving the eigenvalue problem (9). An effective method, in our experience, is to transform the linearized DDAEs into an equivalent system of partial differential equations, and then reduce it through Chebyshev polynomials to a finite-dimensional linear eigenvalue problem. The spectral discretization technique used in this paper is described in [15]. In subsequent steps, if the examined variation alters the power flow solution, the latter is recomputed. Otherwise, if the varying parameters correspond to dynamic devices, the last step is skipped; the operating point is updated from the steady-state DDAEs and the matrices $\mathbf{A}_0$, $\mathbf{A}_1$ and $\mathbf{E}$ are reconstructed. Matrix derivatives are computed numerically using first-order finite differences.

Integration proceeds iteratively until $p = p_{fin}$; firstly, with step size Δp, the parameter is updated as $p_{k+1} = p_k + \Delta p$. Then, the mass matrix $\mathbf{M}(\mathbf{y}_k)$ and right-hand side $\mathbf{h}(\mathbf{y}_k)$ are evaluated, and the state vector is advanced using a numerical integration method. For instance, using forward Euler gives:

$$\mathbf{y}_{k+1} = \mathbf{y}_k + \Delta p\,\mathbf{M}^{-1}(\mathbf{y}_k)\,\mathbf{h}(\mathbf{y}_k) \tag{32}$$

The product $\mathbf{M}^{-1}(\mathbf{y}_k)\,\mathbf{h}(\mathbf{y}_k)$ can be determined through LU decomposition of $\mathbf{M}(\mathbf{y}_k)$.

We note that numerical integration schemes inherently introduce discretization error, which depends on the step size. This error can be practically eliminated by adding a Newton-based corrector step that recomputes the solution within a prescribed tolerance, at additional computational cost.

IV. CASE STUDY

In this section, we apply the continuation-based eigenvalue tracking formulation of Section III to two power system models. First, we consider a modified version of the IEEE 39-bus system [16], and then a real-world-scale model of the Irish transmission system.

A. 39-Bus System

We consider a modified version of the IEEE 39-bus system, wherein the machines at buses 30, 34, 35, 36, 37 are replaced by distributed energy resources (DERs) of equal capacity. Each DER is modeled with an inner current control loop and outer voltage and frequency regulation loops [17].
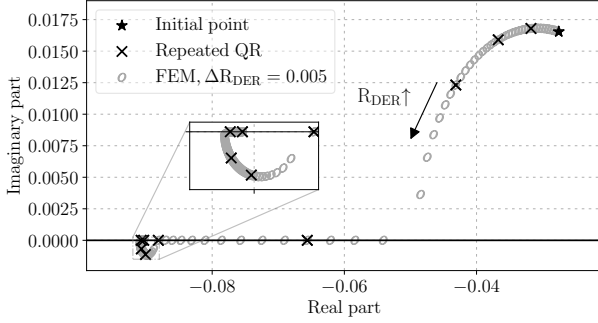
(a) FR mode: increasing the DER frequency controllers' droop constant.
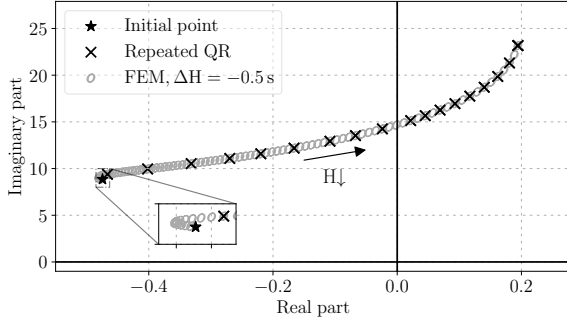
(b) Critical electromechanical mode: Reducing the inertia of the SM at bus 39.

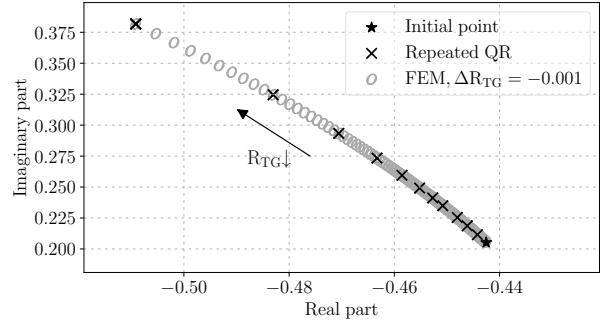Fig. 1: 39-bus system: tracking in the presence of a single delay.

We begin by demonstrating the proposed tracking method on the system's frequency regulation (FR) mode, also referred to as common low-frequency mode in the literature [18], [19]. This is a system-wide mode originating from the dynamics of frequency control loops [14]. For the examined system, the natural frequency of the FR mode is initially 0.005 Hz. To illustrate the process, the frequency control droop constant R_{DER} of the five DERs is varied from 0.05 to 0.5. A single delay of $\tau = 0.01$ s is introduced in the frequency signal of the power system stabilizer (PSS) connected to the synchronous machine (SM) at bus 31. The traced eigenvalue, initially at $-0.0276 + \jmath 0.0165$, follows the trajectory shown in Fig. 1a. Tracking based on (18) accurately captures the trajectory and shows how the oscillatory behavior of the FR mode is progressively suppressed as the relative share of frequency control shifts from the DERs to the SMs. At the point where the complex pair coalesces on the real axis, the eigenvalue becomes defective with algebraic multiplicity 2 and geometric multiplicity 1. This corresponds to a simple quadratic fold [14], [20]. As R_{DER} is further increased, the defective eigenvalue splits into two distinct real eigenvalues. The tracking method inherently follows one of the two emerging branches, as determined by the evolution of (18). In this example, the eigenvalue on the left branch of the fold is traced, and Fig. 1a shows two additional folds occurring along this trajectory. In practice, when such a splitting occurs, the process is reinitialized by recomputing the eigendecomposition of $\mathbf{P}$ and selecting the eigenpair corresponding to the branch of interest.

As a second example, the inertia constant of the system's largest SM is gradually reduced from 50 to 5. Figure 1b illustrates the resulting trajectory of the system's least damped mode, initially located at $-0.4745 \pm \jmath 8.8572$ and corresponding to the local electromechanical mode of the SM at bus 31. Tracking based on (18) shows how the eigenvalue moves as inertia decreases, eventually crossing into the unstable region.
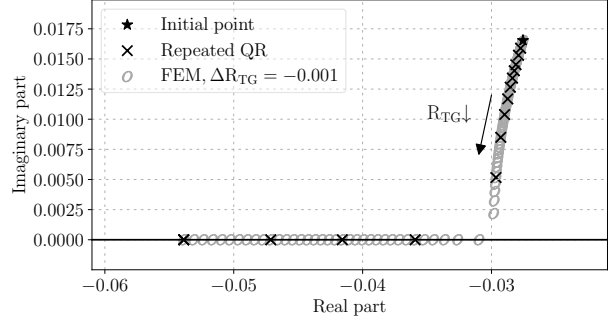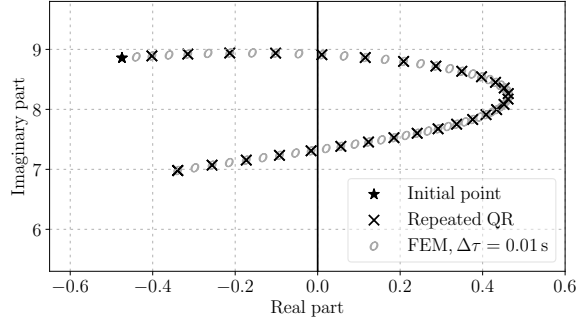

(a) FR mode.

(b) Inter-machine oscillation mode.

Fig. 2: 39-bus system: tracking in the presence of multiple delays.

We next assess the method in the presence of multiple delays. To this end, we introduce delays to the input signals of the system's automatic voltage regulators (AVRs), PSSs and DER frequency and voltage controllers, yielding a total of 20 time-delayed variables. The resulting $\mathbf{P}$ has dimension 558×558. For each delay τ_j, the spectral discretization in [15] uses N Chebyshev nodes in the interval $[-\tau_j, 0]$, which increases the size of $\mathbf{P}$ by $N + 1$. Thus, considering $N = 10$, the dimension of the approximated linear eigenvalue problem grows by 220 compared to the delay-free model. We then trace how variations in the SM droop constants affect the eigenvalues corresponding to (i) the system's FR mode and (ii) the inter-machine mode with the largest participation in the rotor speeds of the SMs at buses 32 and 39, initially located at $-0.4425 \pm \jmath 0.2052$. The calculated trajectories, shown in Fig. 2, confirm that the proposed tracking method accurately captures eigenvalue trajectories in the presence of multiple delays.

We next examine the tracking accuracy when the delay magnitude is treated as the continuation parameter, as described in Section III-C. The analysis focuses on the local electromechanical mode of the SM at bus 31. The delay τ_{PSS} in the input signal of the corresponding PSS is varied from 0.01 to 0.6 s, producing the trajectory shown in Fig. 3a.

As τ_{PSS} increases, the traced eigenvalue becomes progressively less damped and eventually crosses into instability for $\tau_{\text{PSS}} > 0.1$ s. Further increasing τ_{PSS} beyond 0.28 s reverses this trend and eventually leads the system to regain small-signal stability for $\tau_{\text{PSS}} > 0.5$ s. This behavior is further validated via a time-domain simulation, considering a three-phase fault at bus 6, cleared after 80 ms by opening line 5–6. The response of the corresponding SM rotor speed is shown in Fig. 3b and confirms the conclusions drawn by the eigenvalue tracking. In the case of $\tau_{\text{PSS}} = 0.3$ s, the PSS's output introduces a destabilizing negative damping component to the SM's electrical torque, causing the rotor speed to diverge.

Fig. 4: AIITS: tracking poorly damped electromechanical modes in the presence of multiple delays.

(a) Tracing a local electromechanical mode as delay is increased.
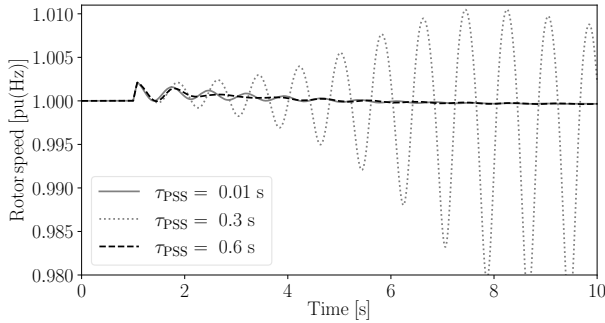
(b) Time-domain simulation for different delay values.

Fig. 3: 39-bus system, SM at bus 31: PSS with input signal delay.

B. Irish System

We assess the scalability of the proposed eigenvalue tracking method using a 1,502-bus dynamic model of the All-Island Irish Transmission System (AIITS). The delay-free DAE model has 1,629 states and 9,897 algebraic variables. Its dimension, 11,526×11,526, renders the use of standard, dense QZ-based eigensolvers impractical. We first examine the accuracy of (18) in tracing poorly damped electromechanical modes of the AIITS. The DDAE model includes 28 delayed variables, affecting voltage and frequency measurements of the system's AVRs and PSSs. The delays, ranging from 0.009 to 0.022 s, increase the dimension of the approximated linear eigenvalue problem to 11,834×11,834. The effect of raising the gains of the system's PSSs from 1.5 to 10, is shown in Fig. 4. Although the examined eigenvalues are tightly clustered
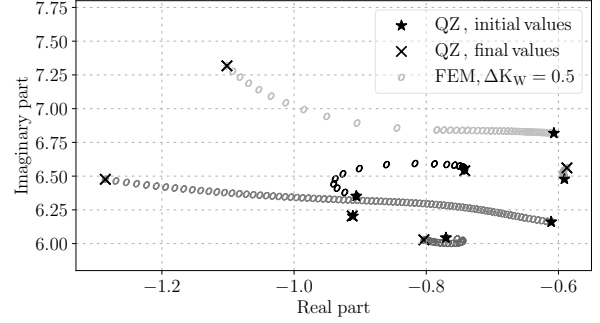
in the complex plane, the proposed approach efficiently traces all of them.

We next apply the formulation in Section III-C to trace the trajectories of the system's poorly damped electromechanical modes, when the time delay of the frequency signal of the PSS, at bus 717 increases from 0.01 to 0.5 s. The results, displayed in Fig. 5, confirm the accuracy of the proposed approach.
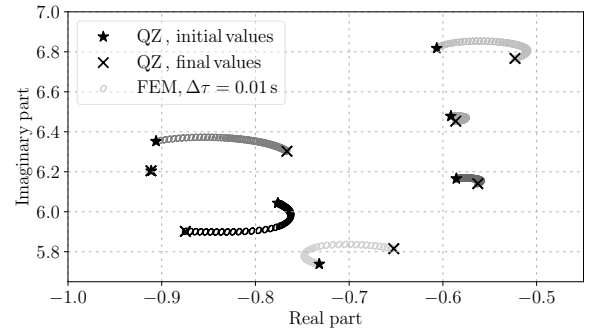

Fig. 5: AIITS, SM at bus 717: increasing PSS input signal delay.

V. CONCLUSION

This paper proposes a continuation-based eigenvalue tracking technique for power systems impacted by time delays. The formulation retains the sparsity of the system's DDAE model and considers a continuation parameter which enables multiple system properties – including delay magnitudes – to be expressed as functions of it and varied simultaneously. Case studies demonstrate the accuracy and computational efficiency of the proposed approach. Future work will focus on applying the proposed approach to guide the design of delay-robust control schemes for DERs.

APPENDIX

In this section, we derive the expressions of $\mathbf{M}$ and $\mathbf{h}$ for the cases considered in Sections III-B, III-C, III-D, i.e., for systems with multiple delays, systems including a varying delay and systems including a WAMS delay.

A. Systems with Multiple Delays

We define the functions $h_r(t) = e^{-s_r t} \cos(s_i t)$ and $h_i(t) = e^{-s_r t} \sin(s_i t)$ and consider the notation $h_r^j = h_r(\tau_j)$ and $h_i^j = h_i(\tau_j)$. By splitting real and imaginary parts of (20) and setting $\mathbf{C} = [\mathbf{A}_j h_r^j]^\intercal$, $\mathbf{S} = [\mathbf{A}_j h_i^j]^\intercal$, $\mathbf{C}_D = [\dot{\mathbf{A}}_j h_r^j]^\intercal$, $\mathbf{S}_D = [\dot{\mathbf{A}}_j h_i^j]^\intercal$, we obtain a system of the form (18), where

$$
\mathbf{h} = \begin{bmatrix} (-s_r\dot{\mathbf{E}} + \dot{\mathbf{A}} + \mathbf{J}_\mu\mathbf{C}_D)\boldsymbol{\phi}_r + (s_i\dot{\mathbf{E}} + \mathbf{J}_\mu\mathbf{S}_D)\boldsymbol{\phi}_i \\ (-s_i\dot{\mathbf{E}} - \mathbf{J}_\mu\mathbf{S}_D)\boldsymbol{\phi}_r + (-s_r\dot{\mathbf{E}} + \dot{\mathbf{A}} + \mathbf{J}_\mu\mathbf{C}_D)\boldsymbol{\phi}_i \\ 0 \\ 0 \end{bmatrix}
$$

$\mathbf{M}_3$ is the same as in (18) and:

$$
\mathbf{M}_1 = \begin{bmatrix} s_r\mathbf{E} - \mathbf{A}_0 - \mathbf{J}_\mu\mathbf{C} & -s_i\mathbf{E} - \mathbf{J}_\mu\mathbf{S} \\ s_i\mathbf{E} + \mathbf{J}_\mu\mathbf{S} & s_r\mathbf{E} - \mathbf{A}_0 - \mathbf{J}_\mu\mathbf{C} \end{bmatrix}
$$

$$
\mathbf{M}_2 = \begin{bmatrix} \mathbf{E}\boldsymbol{\phi}_r + \mathbf{J}_{\tau\mu}(\mathbf{C}\boldsymbol{\phi}_r + \mathbf{S}\boldsymbol{\phi}_i) & -\mathbf{E}\boldsymbol{\phi}_i - \mathbf{J}_{\tau\mu}(\mathbf{C}\boldsymbol{\phi}_r - \mathbf{S}\boldsymbol{\phi}_i) \\ \mathbf{E}\boldsymbol{\phi}_i + \mathbf{J}_{\tau\mu}(\mathbf{C}\boldsymbol{\phi}_r - \mathbf{S}\boldsymbol{\phi}_i) & \mathbf{E}\boldsymbol{\phi}_r + \mathbf{J}_{\tau\mu}(\mathbf{C}\boldsymbol{\phi}_r + \mathbf{S}\boldsymbol{\phi}_i) \end{bmatrix}
$$

with $\mathbf{J}_\mu = [\boldsymbol{I}_r \; \boldsymbol{I}_r \; \dots \; \boldsymbol{I}_r] \in \mathbb{R}^{r \times \mu r}$ and $\mathbf{J}_{\tau\mu} = [\tau_1\boldsymbol{I}_r \; \tau_2\boldsymbol{I}_r \; \dots \; \tau_\mu\boldsymbol{I}_r] \in \mathbb{R}^{r \times \mu r}$; $\boldsymbol{I}_r$ is the $r \times r$ identity matrix.

B. Systems with Delay as Varying Parameter

Splitting real and imaginary parts of (22) and by considering the functions h_r and h_i defined above for $\tau_\ell = p$, we arrive at the form of (18), where in this case:

$$
\mathbf{h} = \begin{bmatrix} \mathbf{h}_1\boldsymbol{\phi}_r + \mathbf{h}_2\boldsymbol{\phi}_i \\ -\mathbf{h}_2\boldsymbol{\phi}_r + \mathbf{h}_1\boldsymbol{\phi}_i \\ 0 \\ 0 \end{bmatrix} \tag{33}
$$

with

$$
\mathbf{h}_1 = -\mathbf{A}_\ell h_r^\ell s_r - \mathbf{A}_\ell h_i^\ell s_i
$$
$$
\mathbf{h}_2 = \mathbf{A}_\ell h_r^\ell s_i - \mathbf{A}_\ell h_i^\ell s_r
$$

$\mathbf{M}_3$ is the same as in (18) and:

$$
\mathbf{M}_1 = \begin{bmatrix} s_r\mathbf{E} - \mathbf{A}_0 - \mathbf{A}_\ell h_r^\ell & -s_i\mathbf{E} - \mathbf{A}_\ell h_i^\ell \\ s_i\mathbf{E} + \mathbf{A}_\ell h_i^\ell & s_r\mathbf{E} - \mathbf{A}_0 - \mathbf{A}_\ell h_r^\ell \end{bmatrix}
$$

$$
\mathbf{M}_2 = \begin{bmatrix} \mathbf{E}\boldsymbol{\phi}_r + p\mathbf{A}_\ell(\boldsymbol{\phi}_r h_r^\ell + \boldsymbol{\phi}_i h_i^\ell) & -\mathbf{E}\boldsymbol{\phi}_i + p\mathbf{A}_\ell(\boldsymbol{\phi}_r h_i^\ell - \boldsymbol{\phi}_i h_r^\ell) \\ \mathbf{E}\boldsymbol{\phi}_i - p\mathbf{A}_\ell(\boldsymbol{\phi}_r h_i^\ell - \boldsymbol{\phi}_i h_r^\ell) & \mathbf{E}\boldsymbol{\phi}_r + p\mathbf{A}_\ell(\boldsymbol{\phi}_r h_r^\ell + \boldsymbol{\phi}_i h_i^\ell) \end{bmatrix}
$$

If the system includes multiple delays, then we also consider the matrices $\mathbf{C}$, $\mathbf{S}$, $\mathbf{J}_\mu$ and $\mathbf{J}_{\tau\mu}$. Splitting real and imaginary parts of (25) we arrive at the form of (18), with $\mathbf{h}$ given by (33) and where in this case

$$
\mathbf{h}_1 = -\mathbf{A}_\ell h_r^\ell s_r - \mathbf{A}_\ell h_i^\ell s_i
$$
$$
\mathbf{h}_2 = \mathbf{A}_\ell h_r^\ell s_i - \mathbf{A}_\ell h_i^\ell s_r
$$

$\mathbf{M}_3$ is the same as in (18) and:

$$
\mathbf{M}_1 = \begin{bmatrix} s_r\mathbf{E} - \mathbf{A}_0 - \mathbf{A}_\ell h_r^\ell - \mathbf{J}_\mu\mathbf{C} & -s_i\mathbf{E} - \mathbf{A}_\ell h_i^\ell - \mathbf{J}_\mu\mathbf{S} \\ s_i\mathbf{E} + \mathbf{A}_\ell h_i^\ell + \mathbf{J}_\mu\mathbf{S} & s_r\mathbf{E} - \mathbf{A}_0 - \mathbf{A}_\ell h_r^\ell - \mathbf{J}_\mu\mathbf{C} \end{bmatrix}
$$

$$
\mathbf{M}_2 = \begin{bmatrix} \mathbf{E}\boldsymbol{\phi}_r + \mathbf{J}_{\tau\mu}(\mathbf{C}\boldsymbol{\phi}_r + \mathbf{S}\boldsymbol{\phi}_i) + \mathbf{A}_\ell p(\boldsymbol{\phi}_r h_r^\ell + \boldsymbol{\phi}_i h_i^\ell) \; \dots \\ \mathbf{E}\boldsymbol{\phi}_i + \mathbf{J}_{\tau\mu}(\mathbf{C}\boldsymbol{\phi}_i - \mathbf{S}\boldsymbol{\phi}_r) - \mathbf{A}_\ell p(\boldsymbol{\phi}_r h_i^\ell - \boldsymbol{\phi}_i h_r^\ell) \; \dots \end{bmatrix}
$$
$$
\begin{bmatrix} \dots -\mathbf{E}\boldsymbol{\phi}_i - \mathbf{J}_{\tau\mu}(\mathbf{C}\boldsymbol{\phi}_i - \mathbf{S}\boldsymbol{\phi}_r) + \mathbf{A}_\ell p(\boldsymbol{\phi}_r h_i^\ell - \boldsymbol{\phi}_i h_r^\ell) \\ \dots \; \mathbf{E}\boldsymbol{\phi}_r + \mathbf{J}_{\tau\mu}(\mathbf{C}\boldsymbol{\phi}_r + \mathbf{S}\boldsymbol{\phi}_i) + \mathbf{A}_\ell p(\boldsymbol{\phi}_r h_r^\ell + \boldsymbol{\phi}_i h_i^\ell) \end{bmatrix}
$$

C. Communication Delays with Noise and Data Dropouts

We set $S_T^r = \Re\{S_T\}$, $S_T^i = \Im\{S_T\}$, $\tilde{\mathbf{S}}_{TD}^r = \Re\{S_{TD}\}\mathbf{A}_1$ and $\tilde{\mathbf{S}}_{TD}^i = \Im\{S_{TD}\}\mathbf{A}_1$. Splitting real and imaginary parts of (31) leads to a system in the form of (18), where in this case $\mathbf{M}_3$ is the same as in (18) and:

$$
\mathbf{h} = \begin{bmatrix} (-s_r\dot{\mathbf{E}} + \dot{\mathbf{A}}_0 + S_T^r\dot{\mathbf{A}}_1)\boldsymbol{\phi}_r + (s_i\dot{\mathbf{E}} - S_T^i\dot{\mathbf{A}}_1)\boldsymbol{\phi}_i \\ -(s_i\dot{\mathbf{E}} - S_T^i\dot{\mathbf{A}}_1)\boldsymbol{\phi}_r + (-s_r\dot{\mathbf{E}} + \dot{\mathbf{A}}_0 + S_T^r\dot{\mathbf{A}}_1)\boldsymbol{\phi}_i \\ 0 \\ 0 \end{bmatrix}
$$

$$
\mathbf{M}_1 = \begin{bmatrix} s_r\mathbf{E} - \mathbf{A}_0 - S_T^r\mathbf{A}_1 & -s_i\mathbf{E} + S_T^i\mathbf{A}_1 \\ s_i\mathbf{E} - S_T^i\mathbf{A}_1 & s_r\mathbf{E} - \mathbf{A}_0 - S_T^r\mathbf{A}_1 \end{bmatrix}
$$

$$
\mathbf{M}_2 = \begin{bmatrix} (\mathbf{E} - \tilde{\mathbf{S}}_{TD}^r)\boldsymbol{\phi}_r + \tilde{\mathbf{S}}_{TD}^i\boldsymbol{\phi}_i & -(\mathbf{E} - \tilde{\mathbf{S}}_{TD}^r)\boldsymbol{\phi}_i + \tilde{\mathbf{S}}_{TD}^i\boldsymbol{\phi}_r \\ (\mathbf{E} - \tilde{\mathbf{S}}_{TD}^r)\boldsymbol{\phi}_i - \tilde{\mathbf{S}}_{TD}^i\boldsymbol{\phi}_r & (\mathbf{E} - \tilde{\mathbf{S}}_{TD}^r)\boldsymbol{\phi}_r + \tilde{\mathbf{S}}_{TD}^i\boldsymbol{\phi}_i \end{bmatrix}
$$

REFERENCES

[1] M. Liu, I. Dassios, G. Tzounas, and F. Milano, "Stability analysis of power systems with inclusion of realistic-modeling WAMS delays," *IEEE Transactions on Power Systems*, vol. 34, no. 1, pp. 627–636, 2018.

[2] I. Zografopoulos, N. D. Hatziargyriou, and C. Konstantinou, "Distributed energy resources cybersecurity outlook: Vulnerabilities, attacks, impacts, and mitigations," *IEEE Systems Journal*, vol. 17, no. 4, pp. 6695–6709, 2023.

[3] R. J. Concepcion, F. Wilches-Bernal, and R. H. Byrne, "Effects of communication latency and availability on synthetic inertia," in *2017 IEEE PES Innovative Smart Grid Technologies Conference (ISGT)*. IEEE, 2017, pp. 1–5.

[4] J. W. Stahlhut, T. J. Browne, G. T. Heydt, and V. Vittal, "Latency viewed as a stochastic process and its impact on wide area power system control signals," *IEEE Transactions on Power Systems*, vol. 23, no. 1, pp. 84–91, 2008.

[5] G. Tzounas, R. Sipahi, and F. Milano, "Damping power system electromechanical oscillations using time delays," *IEEE Transactions on Circuits and Systems I: Regular Papers*, vol. 68, no. 6, pp. 2725–2735, 2021.

[6] F. Milano, I. Dassios, M. Liu, and G. Tzounas, *Eigenvalue Problems in Power Systems*. CRC Press, Taylor & Francis Group, 2020.

[7] P. Kundur, *Power System Stability and Control*. New York: Mc-Grall Hill, 1994.

[8] G. Tzounas, I. Dassios, M. Liu, and F. Milano, "Comparison of numerical methods and open-source libraries for eigenvalue analysis of large-scale power systems," *Applied Sciences*, vol. 10, no. 21, p. 7592, 2020.

[9] L. Dieci and M. J. Friedman, "Continuation of invariant subspaces," *Numerical Linear Algebra with Applications*, vol. 8, no. 5, pp. 317–327, 2001.

[10] O. Liberda and V. Janovský, "Indication of a stability loss in the continuation of invariant subspaces," *Mathematics and Computers in Simulation*, vol. 61, no. 3, pp. 517–524, 2003.

[11] X. Wen and V. Ajjarapu, "Application of a novel eigenvalue trajectory tracing method to identify both oscillatory stability margin and damping margin," *IEEE Transactions on Power Systems*, vol. 21, no. 2, pp. 817–824, 2006.

[12] Q. Mou, Y. Xu, H. Ye, and Y. Liu, "An efficient eigenvalue tracking method for time-delayed power systems based on continuation of invariant subspaces," *IEEE Transactions on Power Systems*, vol. 36, no. 4, pp. 3176–3188, 2021.

[13] C. Li, G. Li, C. Wang, and Z. Du, "Eigenvalue sensitivity and eigenvalue tracing of power systems with inclusion of time delays," *IEEE Transactions on Power Systems*, vol. 33, no. 4, pp. 3711–3719, 2017.

[14] A. Bouterakos, J. McKeon, and G. Tzounas, "On the eigenvalue tracking of large-scale systems," *International Journal of Electrical Power & Energy Systems*, vol. 172, p. 111310, 2025.

[15] C. Li, Y. Chen, T. Ding, Z. Du, and F. Li, "A sparse and low-order implementation for discretization-based eigen-analysis of power systems with time-delays," *IEEE Transactions on Power Systems*, vol. 34, no. 6, pp. 5091–5094, 2019.

[16] Illinois Center for a Smarter Electric Grid (ICSEG), "IEEE 39-Bus System," publish.illinois.edu/smartergrid/ieee-39-bus-system/.

[17] Á. Ortega and F. Milano, "Frequency control of distributed energy resources in distribution networks," *IFAC-PapersOnLine*, vol. 51, no. 28, pp. 37–42, 2018.

[18] F. Wilches-Bernal, J. H. Chow, and J. J. Sanchez-Gasca, "A fundamental study of applying wind turbines for power system frequency control," *IEEE Transactions on Power Systems*, vol. 31, no. 2, pp. 1496–1505, 2016.

[19] A. Moeini and I. Kamwa, "Analytical concepts for reactive power based primary frequency control in power systems," *IEEE Transactions on Power Systems*, vol. 31, no. 6, pp. 4217–4230, 2016.

[20] J. Sun, "Multiple eigenvalue sensitivity analysis," *Linear algebra and its applications*, vol. 137, pp. 183–211, 1990.

Andreas Bouterakos received the Diploma (M.E.) in Electrical and Computer Engineering from the University of Patras, Greece, in 2021. Since September 2023, he has been a Ph.D. candidate with the School of Electrical and Electronic Engineering at University College Dublin, Ireland. His current research interests include stability analysis and automatic control of power systems with high penetration of distributed energy resources.

Georgios Tzounas (M'21) received the Diploma (M.E.) in Electrical and Computer Engineering from the National Technical Univ. of Athens, Greece, in 2017, and the Ph.D. from University College Dublin (UCD), Ireland, in 2021. In Jan.-Apr. 2020, he was a visiting researcher at Northeastern Univ., Boston, MA. From Oct. 2020 to Apr. 2023, he was a postdoctoral researcher with UCD (2020-2022) and ETH Zürich (2022-2023). Since Apr. 2023, he has been an Assistant Professor with the School of Electrical and Electronic Engineering at UCD. His primary research area is power system dynamics.